Performance Comparison Between Mho Elements and Incremental Quantity-Based Distance Elements

Gabriel Benmouyal, Normann Fischer, and Brian Smyth
Schweitzer Engineering Laboratories, Inc.

This paper was presented at the 70th Annual Conference for Protective Relay Engineers and can be accessed at: https://doi.org/10.1109/CPRE.2017.8090043.

For the complete history of this paper, refer to the next page.

Presented at the
71st Annual Georgia Tech Protective Relaying Conference
Atlanta, Georgia
May 3–5, 2017

Previously presented at the
70th Annual Conference for Protective Relay Engineers, April 2017

Previous revised edition released October 2016

Originally presented at the
43rd Annual Western Protective Relay Conference, October 2016

Performance Comparison Between Mho Elements and Incremental Quantity-Based Distance Elements

Gabriel Benmouyal, Normann Fischer, and Brian Smyth, *Schweitzer Engineering Laboratories, Inc.*

***Abstract*—Mho elements constitute the main component of transmission line protection in North America and many countries overseas. Distance elements based on incremental quantities and derived from the same base equations as mho elements emerged about two decades ago as a way to improve the speed of distance elements. This paper compares the intrinsic protective properties of mho and incremental distance elements, irrespective of the ways they are implemented.**

I. Introduction

Mho distance elements have been the mainstay of impedance-based transmission line protection for decades, and their use is practically standard practice in North America and internationally. Distance elements based on incremental quantities (called simply "incremental distance elements" in this paper) and derived from the same base equations as mho elements as shown in this paper, have recently been used in high- and ultra-high-speed applications in parallel with, or independent of, mho elements. This paper provides an answer to this question: Do incremental distance elements perform exactly the same as conventional mho distance elements? In other words, is the incremental distance element more sensitive or less sensitive than a conventional distance element?

For the purpose of performance comparison between the two elements, this paper makes extensive use of their respective characteristics in the loop impedance plane. The paper discusses the respective limitations imposed by the requirements for each element's implementation, such as voltage polarization using voltage memory for conventional mho elements and using incremental or delta quantities for incremental distance elements. Applications such as the protection of series-compensated lines require conventional mho distance elements to be polarized with the correct voltage (voltage memory) in order to perform correctly. Incremental distance elements, on the other hand, require the calculation of superimposed voltage and current components that are processed by delta filters. Incremental distance elements only perform correctly if they are supplied with the correct incremental voltage and current components.

The focus of this paper is not how to implement a conventional mho or incremental distance element in terms of filter design and speed of operation. The main focus is the performance of the two distance elements with respect to providing protection for a transmission line.

The derivations of the incremental distance element equations are a result of the superposition principle applied to power systems: a faulted network can be resolved by defining a prefault and a pure-fault circuit [1]. This paper begins by revisiting this important principle.

II. The Superposition Principle Applied to Faulted Power Networks

A. The Superposition Principle Applied to Three-Phase Faults

Consider the elementary power system shown in Fig. 1. Assume that a three-phase fault occurs at a distance *d* in per unit (pu) of the line length from Bus L.

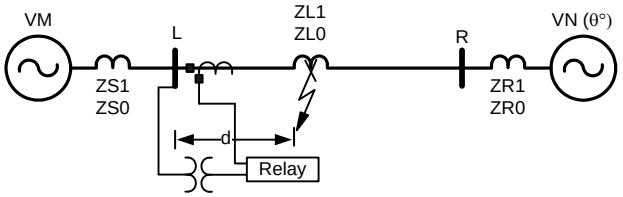

Fig. 1. Elementary power system network

The superposition principle can be applied to resolve the equations of the faulted circuit voltages and currents [1]. Let Ef_A be the A-phase prefault voltage at the fault point on the line. The value of this voltage is provided by (1).

$$Ef_A = VM - (ZSl + d \bullet ZL1) \bullet I_{LD} \quad (1)$$

The A-phase prefault current (IA_{PF}), also called load current (I_{LD}), is given in (2).

$$I_{LD} = IA_{PF} = \frac{VM - VN}{(ZSl + ZR1 + ZL1)} \quad (2)$$

Fig. 2 represents the pure-fault sequence network for three-phase faults [1]. The driving voltage Ef_A corresponds to the A-phase prefault voltage at the fault location. R_F is the fault resistance. The quantities existing in the prefault network and belonging to the pure-fault circuit are represented with a Δ prefix, which represents a change or an increment. The prefix Δ, in front of any voltage or current belonging to the pure-fault network, indicates that the corresponding change in voltage or current is due to the fault only.

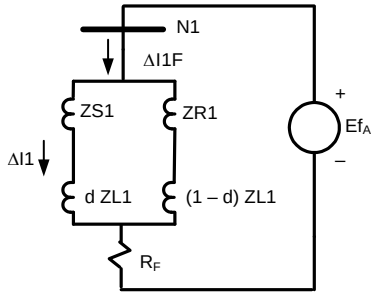

Fig. 2. Pure-fault sequence network of a three-phase fault

Any voltage or current of the faulted circuit can be resolved as the sum of the prefault voltage or current and the pure-fault circuit voltage or current increment, as shown in (3).

$$\begin{aligned} V &= V_{PF} + \Delta V \\ I &= I_{PF} + \Delta I \end{aligned} \tag{3}$$

In Fig. 2, the incremental positive-sequence current at the relay location is shown with the Δ prefix because it is a pure-fault current. It is expressed in (4) as a function of the positive-sequence current at the fault point.

$$\Delta I1 = C1 \bullet \Delta I1F \tag{4}$$

In (4), C1 is the positive-sequence current distribution factor. It is expressed in (5) as a function of the network impedances.

$$C1 = \frac{(1-d) \bullet ZL1 + ZR1}{ZS1 + ZL1 + ZR1} \tag{5}$$

By virtue of the superposition principle, the positive-sequence current at the relay is provided by the sum of the prefault current plus the incremental positive-sequence current. This is shown in (6).

$$I1 = I_{LD} + \Delta I1 = \left(\frac{1}{3}\right) \bullet (IA + a \bullet IB + a^2 \bullet IC) \tag{6}$$

In (6), *a* is the operator defined in (7).

$$a = 1\angle 120° \tag{7}$$

For three-phase faults, the relationship shown in (8) between the A-phase voltage and current is at the relay location.

$$VA = d \bullet ZL1 \bullet IA + R_F \bullet \Delta I1F \tag{8}$$

By applying (3) to (8), the relationship between the prefault and pure-fault A-phase quantities can be derived as shown in (9).

$$\begin{aligned} Ef_A &= VA_{PF} - d \bullet ZL1 \bullet I_{LD} = \\ &-\Delta VA + d \bullet ZL1 \bullet \Delta IA + R_F \bullet \Delta I1F \end{aligned} \tag{9}$$

Expressions equivalent to (8) and (9) can also be derived for the B- and C-phases.

The pure-fault or incremental A-phase current at the relay is equal to the positive-sequence current distribution factor multiplied by the pure-fault positive-sequence current at the fault, as shown in (10).

$$\Delta IA = C1 \bullet \Delta I1F \tag{10}$$

The incremental A-phase voltage ΔVA is as shown in (11).

$$\Delta VA = -ZS1 \bullet C1 \bullet \Delta I1F = -ZS1 \bullet \Delta IA \tag{11}$$

B. The Superposition Principle Applied to Single-Phase-to-Ground Faults

The analysis carried out in Section II, Subsection A for the three-phase fault sequence network can be applied to any fault-type sequence network. Fig. 3 shows the pure-fault sequence network for single A-phase-to-ground faults.

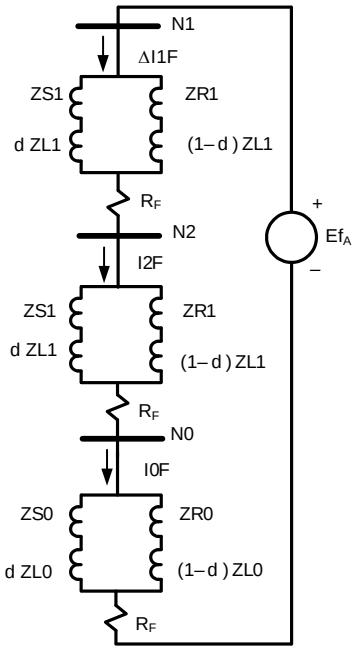

Fig. 3. Pure-fault sequence network of an A-phase-to-ground fault

For the single A-phase-to-ground fault network represented in Fig. 3, the relationship between the phase voltage and the loop current at the relay during the fault is provided by [2] and shown in (12).

$$VA = d \bullet ZlL \bullet (IA + K_0 \bullet I0) + 3R_F \bullet \Delta I1F \tag{12}$$

In (12), the zero-sequence compensation factor K_0 is expressed as a function of the line impedances as shown in (13).

$$K_0 = \frac{ZL0 - ZL1}{ZL1} \tag{13}$$

Applying the superposition principle to the voltage VA and current IA results in (14).

$$\begin{aligned} VA &= VA_{PF} + \Delta VA \\ IA &= IA_{PF} + \Delta IA = I_{LD} + \Delta IA \end{aligned} \tag{14}$$

Substituting the expressions of VA and IA as given by (14) into (12) results in (15).

$$\begin{aligned} &VA_{PF} + \Delta VA = \\ &d \bullet Z1L \bullet ((I_{LD} + \Delta IA) + K_0 \bullet I0) + 3R_F \bullet \Delta I1F \end{aligned} \tag{15}$$

From (15), the relationship between the prefault and pure-fault quantities for the single A-phase-to-ground faults can be derived as shown in (16).

$$\begin{aligned} &Ef_A = VA_{PF} - d \bullet ZL1 \bullet I_{LD} = \\ &-\Delta VA + d \bullet ZL1 \bullet (\Delta IA + K_0 \bullet I0) + 3R_F \bullet \Delta I1F \end{aligned} \tag{16}$$

In (16), ΔVA (the incremental A-phase voltage) and ΔIA (the incremental current) can be expressed as shown in (17).

$$\begin{aligned} \Delta VA &= -(2 \bullet C1 \bullet ZS1 + C0 \bullet ZS0)\Delta I1F \\ \Delta IA &= (2 \bullet C1 + C0)\Delta I1F \end{aligned} \tag{17}$$

In (17), the zero-sequence current distribution factor C0 is defined as shown in (18).

$$C0 = \frac{(1-d) \bullet ZL0 + ZR0}{ZS0 + ZL0 + ZR0} \tag{18}$$

C. The Superposition Principle Applied to Double-Phase and Double-Phase-to-Ground Faults

The same analysis can be carried out for a double-phase fault. The pure-fault sequence network for a B-phase-to-C-phase fault is shown in Fig. 4.

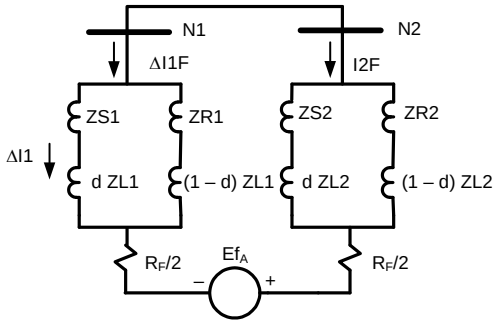

Fig. 4. Pure-fault sequence network for a phase-to-phase fault

From Fig. 4, the relationship between the prefault and pure-fault voltage and current quantities with respect to the A-phase is provided by (19).

$$\begin{aligned} &Ef_A = VA_{PF} - d \bullet ZL1 \bullet I_{LD} = \\ &(ZS1 + d \bullet ZL1) \bullet (C1 \bullet \Delta I1F \bullet -C2 \bullet I2F) + \frac{R_F}{2}(\Delta I1F - I2F) \end{aligned} \tag{19}$$

where:

$$C2 = C1 = \frac{(1-d) \bullet ZL1 + ZR}{ZS1 + ZL1 + ZR1} \tag{20}$$

For a phase-to-phase fault, (21) is true.

$$\Delta I1F = -I2F \tag{21}$$

Therefore, (19) can be reduced to (22).

$$Ef_A = (ZS1 + d \bullet ZL1) \bullet 2C1 \bullet \Delta I1F + R_F \Delta I1F \tag{22}$$

Equivalent relationships can be derived for the B- and C-phases. For the B-phase, the voltages and currents have to be multiplied by a^2, with a defined by (7). For the C-phase, they have to be multiplied by a.

III. Conventional Mho Element Implementation

A. Implementation of Mho Elements

In a transmission line relay, six impedance loops are required to cover all the possible shunt-type faults [2] [3] [4] [5]. Each of these fault loops has its own distance element. The six loops correspond to the three phase-to-ground fault loops (AG, BG, and CG) and the three phase-to-phase fault loops (AB, BC, and CA).

Protecting a fault loop with a mho element requires an operating quantity S_{OP} and a polarizing quantity S_{POL} as defined in (23).

$$\begin{aligned} S_{OP} &= r \bullet ZL1 \bullet IR - VR \\ S_{POL} &= V_{POL} \end{aligned} \tag{23}$$

where:

r is the element reach

IR is the particular loop current

VR is the particular loop voltage

V_{POL} is a polarizing voltage

One of the most popular polarization methods is to use positive-sequence voltage memory (PSVM), typically processed through a dedicated filter [5]. Polarization with positive-sequence voltage (PSV) is readily accessible as an alternative, but it results in decreased sensitivity to resistive faults, problematic performance with three-phase bolted faults, and voltage inversion with series compensation.

The mho element asserts when the scalar product SP between the operating quantity and the polarizing quantity is positive or when it satisfies the inequality in (24).

$$SP = real\left[(r \bullet ZL1 \bullet IR - VR) \bullet conj(V_{POL})\right] \geq 0 \qquad (24)$$

In (24), *real* represents "real part of" and *conj* stands for "complex conjugate of."

Performing a scalar product is tantamount to implementing an angle comparator: if the angle between the polarizing quantity and the operating quantity becomes smaller than 90 degrees, then the element asserts.

B. Alternative Solution to Using the Scalar Product

An alternate solution to performing the scalar product in (24) is to calculate a distance *m*, as indicated in (25), and then compare the calculated *m* value with the different reach setting thresholds [5].

$$m = \frac{real\left[VR \bullet conj(V_{POL})\right]}{real\left[ZL1 \bullet IR \bullet conj(V_{POL})\right]} \qquad (25)$$

The advantage of this alternative solution is that *m* is calculated once for all the fault loops and is compared with the reach settings of any of the zones. Another advantage for small values of fault resistance is that *m* equals a value close to the distance to the fault *d*.

C. Loop Apparent Impedance and Distance Element Characteristic in the Loop Impedance Plane

When distance protection is applied to the elementary power network shown in Fig. 1, the apparent impedance seen from Bus L and calculated for any of the six possible faulted impedance loops can be expressed by the generic equation (26), assuming that a prefault load current exists [2].

$$Z_{APP} = \frac{VR}{IR} = d \bullet ZL1 + R_F \frac{K_R}{K_I} \qquad (26)$$

In (26), K_I is the ratio of the faulted loop current over the change of the same current, as shown in (27).

$$K_I = \frac{IR}{IR - IR_{PF}} = \frac{IR}{\Delta IR} \qquad (27)$$

K_R is a factor involving network parameters. Table I provides the expression of K_R as a function of the fault type [2]. Table II in [2] provides additional information about the location of the fault resistance R_F for the different fault types.

TABLE I
EXPRESSIONS OF K_R

Fault Type	K_R
Single-phase-to-ground (K_{RAG}, K_{RBG}, K_{RCG})	$\frac{3}{2Cl + C0(1 + K_0)}$
Double-phase (K_{RAB}, K_{RBC}, K_{RCA})	$\frac{1}{2 \bullet Cl}$
Three-phase (K_{RABC})	$\frac{1}{Cl}$

The loop apparent impedance with no load current ($I_{LD} = 0$) will simply be (26) with $K_I = 1$, as shown in (28).

$$Z_{APP\_NLD} = d \bullet ZL1 + R_F \bullet K_R \qquad (28)$$

When applied to conventional mho elements, the apparent impedance can always be calculated and the characteristics always exist in the impedance plane, whether or not the network is healthy. When the apparent impedance with respect to a particular impedance loop plots within the area delimited by the corresponding element characteristic in the impedance plane, the conventional mho element operates [3] [4]. The same is not true with incremental distance elements; the characteristic only exists in the impedance plane if the incremental voltage and current quantities are non-zero. Subsequent sections in the paper explain that, following a fault, the incremental quantities are non-zero only for a short interval of time. Checking the location of the apparent impedance against any characteristic in the impedance plane can only be performed during that short interval of time and cannot be performed when the incremental quantities are zero. This paper compares the characteristics of the conventional mho and incremental distance elements as the base representation in order to evaluate their respective performances.

IV. DISTANCE ELEMENT BASED ON INCREMENTAL QUANTITIES

A. Ground Incremental Distance Element

Starting with (16), which provides the relationship between the prefault and pure-fault quantities for single A-phase-to-ground faults, we equate the distance to the fault *d* with the reach *r* as shown in (29).

$$\begin{aligned} VA_{PF} - r \bullet ZL1 \bullet I_{LD} = \\ -\Delta VA + r \bullet ZL1 \bullet (\Delta IA + K_0 \bullet I0) + 3R_F \bullet \Delta I1F \end{aligned} \qquad (29)$$

Assuming that R_F is zero, two new quantities can be defined: Vf_{AG} and Vd_{AG}. Equation (29) can then be rewritten as shown in (30).

$$\begin{aligned} Vf_{AG} &= VA_{PF} - r \bullet ZlL \bullet IA_{PF} \\ Vd_{AG} &= -\Delta VA + r \bullet ZlL \bullet (\Delta IA + K_0 \bullet I0) \end{aligned} \tag{30}$$

Vf_{AG} is simply the prefault voltage at the reach location. Vd_{AG} can be defined as an incremental voltage drop at the reach location. It is importance to note that Ef_{AG} and Vf_{AG} are defined differently. Ef_{AG} is the prefault A-phase voltage at the fault location, and Vf_{AG} is the prefault A-phase voltage at the reach location. Equivalent expressions are defined for B- or C-phase-to-ground faults.

Assuming an R_F equal to zero and a reach *r* equal to 80 percent, Fig. 5 shows the locus of the absolute values of Vf_{AG} (solid red line) and Vd_{AG} (solid blue line) as the fault is applied with the distance *d* varying from 0 to 1 pu of the line length for an element installed on Bus L of the power circuit in Fig. 6. Obviously, Vf_{AG} is a constant and the incremental voltage drop Vd_{AG} is decreasing. From Fig. 5, the three conditions in (31) can be inferred.

$$\begin{aligned} d < r \quad &\Rightarrow \quad |Vd_{AG}| > |Vf_{AG}| \\ d = r \quad &\Rightarrow \quad |Vd_{AG}| = |Vf_{AG}| \\ d > r \quad &\Rightarrow \quad |Vd_{AG}| < |Vf_{AG}| \end{aligned} \tag{31}$$

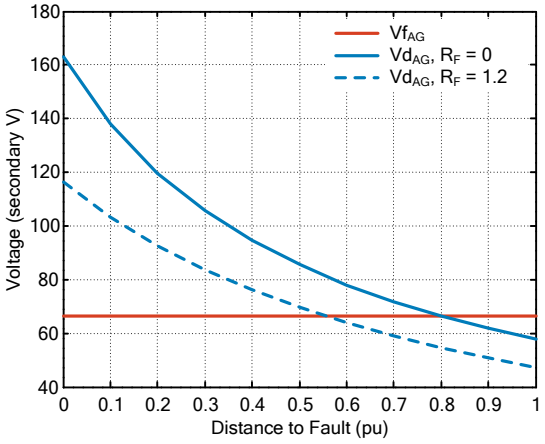

Fig. 5. Prefault voltage at the reach location and incremental voltage drop as seen from Bus L of the circuit in Fig. 6 for an A-phase-to-ground fault

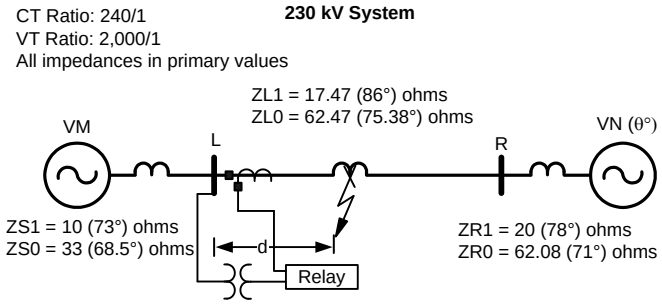

Fig. 6. Single-line, 230 kV system

The three conditions in (31) determine the principle for fault detection using a distance element based on incremental quantities. Whereas with a conventional mho element, the sign of a scalar product between an operating and a polarizing vector determines if there is a fault or not, a magnitude comparison between a prefault voltage at the reach location and an incremental voltage drop at the reach location plays the same role with a distance element based on incremental quantities. Vd_{AG} can be called an operating quantity and Vf_{AG} can be called a restraining quantity. The element asserts when the operating quantity is greater than the restraining quantity.

In Fig. 5, Vd_{AG} has also been plotted with the dashed blue line for an R_F of 1.2 ohms secondary. Given that Vf_{AG} does not change, as the fault resistance increases, the incremental distance element starts to underreach. The element covers only approximately 55 percent of the power line when R_F equals 1.2 ohms. If we keep increasing R_F, a maximum resistance value will be reached for which the fault will not be detected at distance *d* equal to zero.

In Fig. 6, impedances are shown in primary values, but they are indicated in secondary values throughout the text and in all other figures.

B. Phase Incremental Distance Element

The derivation for phase incremental distance elements is identical to the one performed for ground incremental distance elements. For A-phase-to-B-phase faults or A-phase-to-B-phase-to-ground faults, the prefault voltage at the reach point and the incremental voltage drop are as shown in (32).

$$\begin{aligned} Vf_{AB} &= (VA_{PF} - VB_{PF}) - r \bullet ZlL \bullet (IA_{PF} - IB_{PF}) \\ Vd_{AB} &= -(\Delta VA - \Delta VB) + r \bullet ZlL \bullet (\Delta IA - \Delta IB) \end{aligned} \tag{32}$$

Equivalent expressions are derived for B-phase-to-C-phase and C-phase-to-A-phase faults.

V. Mho and Incremental Distance Element Characteristics in the Loop Impedance Plane

A. Case of Three-Phase Faults

1) Mho Element Characteristic for Three-Phase Faults With No Load

The representation of the conventional mho expansion or its characteristic in the loop impedance plane depends on the polarization type. It is well known that the maximum expansion occurs when the PSVM is used for the polarizing voltage [6]. For three-phase faults, any phase voltage and current or any difference of phase voltage and current can be used to determine the characteristic. For simplicity, the A-phase voltage and current are used, as shown in (33).

$$\begin{aligned} S_{OP\_ABC} &= r \bullet ZL1 \bullet IA - VA \\ S_{POL\_ABC} &= VA1_{MEM} \end{aligned} \tag{33}$$

In (33), $VA1_{MEM}$ is the PSVM referenced to the A-phase. In order to define the characteristic circle in the impedance plane, both the operating S_{OP} and polarizing S_{POL} quantities need to be divided by the fault current IA, as shown in (34).

$$\begin{aligned}\frac{S_{OP\_ABC}}{IA} &= S'_{OP\_ABC} = r \bullet ZL1 - \frac{VA}{IA} \\ \frac{S_{POL\_ABC}}{IA} &= S'_{POL\_ABC} = \frac{VA1_{MEM}}{IA}\end{aligned} \tag{34}$$

The ratio of VA over IA is simply the apparent impedance measured at the relay. For a system with no load ($I_{LD} = 0$), the ratio is as given by (35).

$$\frac{VA}{\Delta IA} = Z_{APP\_NLD} = d \bullet ZL1 + \frac{R_F}{C1} \tag{35}$$

$VA1_{MEM}$ is equal to the prefault voltage VA_{PF}. Starting with (9) and applying the identity in (11) results in (36) for a system with no load.

$$VA1_{MEM} = VA_{PF} = (ZS1 + d \bullet ZL1) \bullet \Delta IA + R_F \bullet \Delta I1F \tag{36}$$

Dividing (36) by ΔIA produces (37).

$$\begin{aligned}\frac{VA1_{MEM}}{\Delta IA} &= (ZS1 + d \bullet ZL1) + \frac{R_F}{C1} \\ &= ZS1 + Z_{APP\_NLD}\end{aligned} \tag{37}$$

The operating and polarizing quantities in (34) for a system with no load can then be expressed as shown in (38).

$$\begin{aligned}S'_{OP\_ABC} &= r \bullet ZL1 - Z_{APP\_NLD} \\ S'_{POL\_ABC} &= ZS1 + Z_{APP\_NLD}\end{aligned} \tag{38}$$

The operating and polarizing vectors in (38) translate geometrically into the well-known circle characteristic, which is also commonly dubbed the mho dynamic expansion because the circle does not cross the origin point, as shown in Fig. 7. The circle diameter is the segment corresponding to the sum of ZS1 plus the reach *r* multiplied by ZL1. The circle center is at the middle of this segment. The operating vector dZ is perpendicular to the polarizing vector $ZS1 + Z_{APP\_NLD}$, where the apparent impedance Z_{APP_NLD} falls exactly on the diameter of the circle.

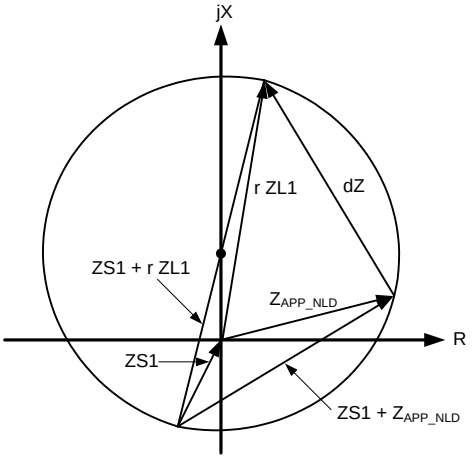

Fig. 7. Expanded mho element characteristic for three-phase faults with PSVM polarization

When PSV is used as the polarizing quantity, the operating and polarizing quantities in (34) are expressed as (39).

$$\begin{aligned}S'_{OP\_ABC} &= r \bullet ZL1 - Z_{APP\_NLD} \\ S'_{POL\_ABC} &= Z_{APP\_NLD}\end{aligned} \tag{39}$$

Using PSV for the polarizing quantity results in a characteristic corresponding to the well-known, self-polarized mho circle, as shown in Fig. 8. In this instance, the mho circle encompasses the origin point. The expansion of the PSVM-polarized mho element is determined by comparing it with the PSV-polarized mho element.

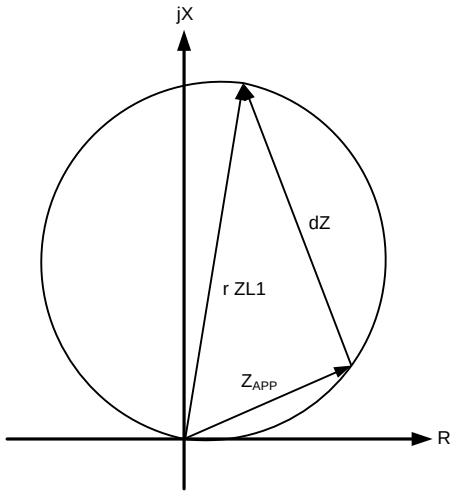

Fig. 8. Mho element characteristic for three-phase faults with PSV polarization

In many applications, PSVM polarization is implemented using a memory filter. The output immediately after the fault inception is the prefault PSV, and the voltage memory slowly decays until the filter output reaches the value of the present PSV [6]. Under these conditions, following a three-phase fault, we must understand that the mho element characteristic starts with the maximum expansion, as shown in Fig. 7, and ends up with the self-polarization characteristic of Fig. 8 [6]. This feature allows the element to detect bolted three-phase faults and close to the relaying point when the PSV goes to zero following the fault.

2) Impact of Load on the Mho Element Characteristic

When load is taken into account, $VA1_{MEM}$ is again equal to VA_{PF}, and (36) has to be rewritten as shown in (40).

$$VA1_{MEM} = VA_{PF} = ZS1 \bullet \Delta IA + d \bullet ZL1 \bullet IA + R_F \bullet \Delta I1F \tag{40}$$

As a result, (38) becomes equal to (41).

$$\begin{aligned}\frac{S_{OP\_ABC}}{IA} &= S'_{OP\_ABC} = r \bullet ZL1 - \frac{VA}{IA} = r \bullet ZL1 - Z_{APP} \\ \frac{S_{POL\_ABC}}{IA} &= S'_{POL\_ABC} = \frac{VA1_{MEM}}{IA} = \frac{ZS1}{K_I} + Z_{APP}\end{aligned} \tag{41}$$

When load is taken into account, the mho element characteristic at no load is modified so that the source impedance behind the relay has to be divided by K_I, and the apparent impedance is the one incorporating the factor K_I, as provided by (27).

3) Incremental Distance Element Characteristic in the Loop Impedance Plane for Three-Phase Faults

Starting with the expression of Ef_A in (9), the incremental distance element characteristic in the impedance plane for three-phase faults can be obtained by expressing the prefault voltage at the fault location and the incremental voltage drop at the element reach for the A-phase as shown in (42).

$$\begin{aligned} Ef_A &= -\Delta VA + d \bullet ZL1 \bullet \Delta IA + R_F \bullet \Delta I1F \\ Vd_A &= -\Delta VA + r \bullet ZL1 \bullet \Delta IA \end{aligned} \tag{42}$$

As was done for the mho element, both terms of (42) are divided by ΔIA. By virtue of applying identities (10), (11), and (28), the result is (43).

$$\begin{aligned} Ef_A^{'} &= \frac{Ef_A}{\Delta IA} = ZS1 + d \bullet ZL1 + \frac{R_f}{C1} = ZS1 + Z_{APP\_NLD} \\ Vd_A^{'} &= \frac{Vd_A}{\Delta IA} = ZS1 + r \bullet Z1L \end{aligned} \tag{43}$$

Because the incremental distance element is an amplitude comparator as expressed in (31), it is necessary to have the next condition shown in (44) for the element to pick up.

$$\left|ZS1 + r \bullet Z1L\right| \geq \left|ZS1 + Z_{APP\_NLD}\right| \tag{44}$$

The vector magnitude inequality in (44) indicates that the incremental distance element characteristic in the impedance plane during a three-phase fault is simply an offset mho element; the center coordinates (x_0, y_0) and radius *R* are provided by (45).

$$\begin{aligned} x_0 &= -\text{real}(ZS1) \\ y_0 &= -\text{imag}(ZS1) \\ R &= \text{abs}(ZS1 + r \bullet ZL1) \end{aligned} \tag{45}$$

In order for the three-phase fault incremental distance element to pick up, the apparent impedance with no load corresponding to (28) has to fall inside the circle characteristic corresponding to (45). As noted previously, in order to carry out this check, the incremental voltage and current (ΔVA and ΔIA) have to be non-zero.

4) Impact of the Load on the Incremental Distance Element Characteristics

When the load current I_{LD} is non-zero, the three-phase fault incremental distance characteristic does not change in the loop impedance plane. It is therefore immune to load variations.

5) Comparison of Mho and Incremental Distance Element Characteristics for Three-Phase Faults

With zero load, both the mho and incremental distance elements have the same apparent impedance in the loop impedance plane. With a reach *r* equal to 80 percent of the line length, Fig. 9 shows the following three characteristics for a distance element installed at Bus L of the network in Fig. 6:

- The mho element characteristic with PSVM polarization (solid blue line).
- The mho element characteristic with PSV polarization (dashed blue line).
- The incremental distance element characteristic (solid red line).

Fig. 9 shows that the incremental distance element has an intrinsic expansion that is superior to the mho element even with the best possible polarization (PSVM polarization).

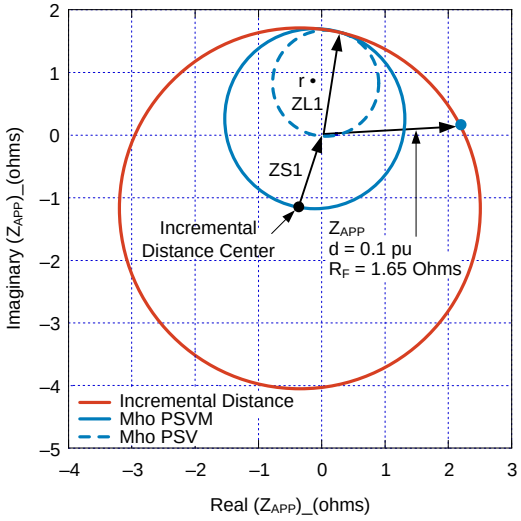

Fig. 9. Three-phase fault mho and incremental distance element characteristics for a relay installed at Bus L of the network in Fig. 6

Another significant aspect to evaluate is the impact of each characteristic with respect to the resistance coverage of each element as a function of fault distance. This resistance coverage is represented in Fig. 10 for all of the elements for the network in Fig. 6 with no load, as seen by the elements installed at Bus L. Obviously, the larger characteristic for the incremental distance function translates into a greater resistance coverage and, consequently, improved sensitivity. As could be expected, resistance coverage of the mho element with PSV polarization is degraded for faults close to the substation.

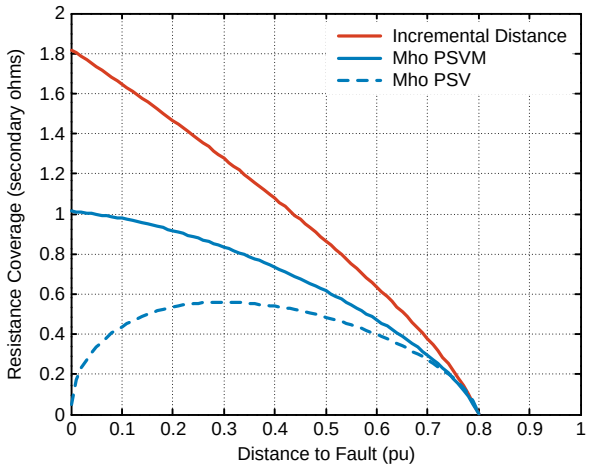

Fig. 10. Resistance coverage for three-phase faults as a function of the distance to the fault

For the network in Fig. 6, when the distance to the fault is 0.1 pu, the maximum fault resistance that can be detected by the three-phase incremental distance element (as indicated in Fig. 10) is 1.65 ohms. The loop apparent impedance, using the A-phase voltage and current, is verified in (46).

$$Z_{APP\_NLD}(d = 0.1,\ R_F = 1.6465) = \frac{VA}{\Delta IA} = d \bullet ZL1 + \frac{R_F}{Cl} = (2.199 + j0.147)\ \Omega \quad (46)$$

This apparent impedance is plotted in Fig. 9 and falls exactly on the incremental distance element characteristic circle. This verifies that the characteristic is valid. Should R_F be increased, the loop apparent impedance would fall outside the characteristic circle, and this would be an indication that the detector does not see the fault any longer, as would be expected.

It might be expected that the resistance coverage of both elements, conventional mho and incremental distance, would be smaller if the line length were reduced. Fig. 11 represents the new characteristics for both elements, with the line impedance reduced to 1/10 of its original value. Note that both characteristics are much smaller in the impedance plane. This translates into significantly smaller resistance coverage, as shown in Fig. 12. Note that the incremental distance element still has superior coverage.

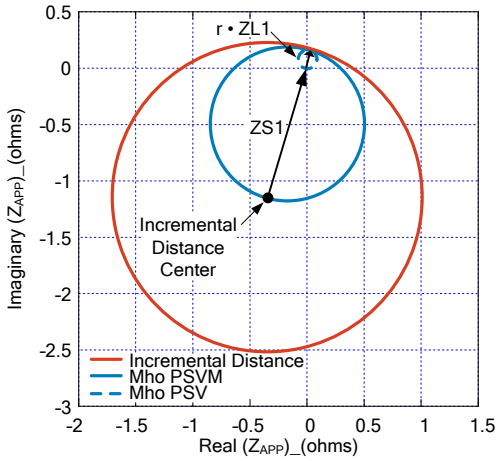

Fig. 11. Three-phase fault mho and incremental distance element characteristics with ZL1 equal to 1/10 of its original value

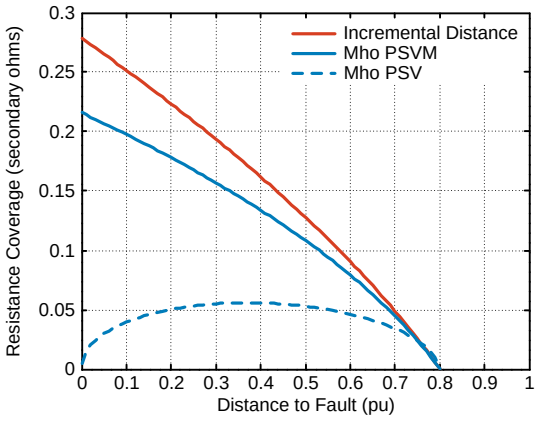

Fig. 12. Resistance coverage for three-phase faults with ZL1 equal to 1/10 its original value as a function of the distance to the fault

If the source impedance behind the relay were very small compared with the line impedance, the mho element characteristic would be very close to the origin point and the resistance coverage for faults close to Bus L would be very small, even with a voltage polarization with a memory effect. Fig. 13 shows both characteristics with a value of ZS1 equal to 1/20 of its original value. The source impedance is very small and is now located between the incremental distance element characteristic center and the origin. The mho element characteristics with either PSV or PSVM polarization have become almost identical, and the voltage memory does not help much in this case. Fig. 14 shows the resistance coverage for both elements. Even if the mho element lost its capacity to cover resistive faults close to the origin, the incremental distance is still capable of covering practically the same amount of resistance as it does in Fig. 10. The mho element resistance coverage is substantially degraded with faults close to the substation, even with the best possible PSVM polarization.

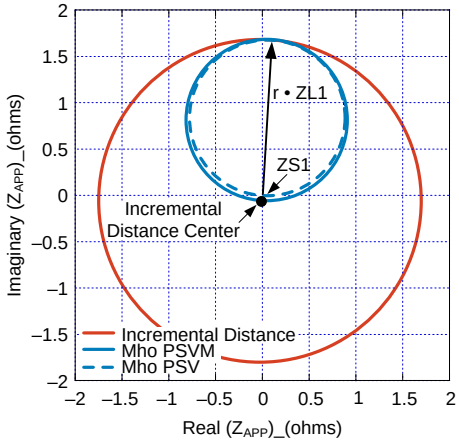

Fig. 13. Three-phase fault mho and incremental distance element characteristics with ZS1 equal to 1/20 its original value

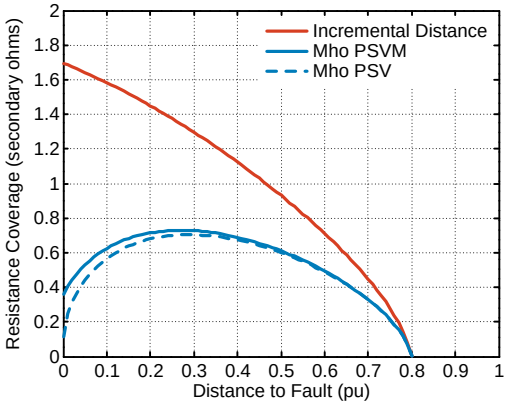

Fig. 14. Resistance coverage for three-phase faults with ZS1 equal to 1/20 its original value as a function of the distance to the fault

B. Case of Single-Phase Faults

1) Mho Element Characteristic for Single A-Phase-to-Ground Faults With PSVM Polarization

For a single A-phase-to-ground fault with PSVM polarization, the conventional mho distance element using a

phase-angle comparator has the operating and polarizing quantities shown in (47).

$$\begin{aligned} S_{OP\_AG} &= r \bullet ZL1 \bullet IR_{AG} - VA = r \bullet ZL1 \bullet (IA + K_0 I0) - VA \\ S_{POL\_AG} &= VA1_{MEM} \end{aligned} \tag{47}$$

Using the same method for three-phase faults and assuming a system with no load ($I_{LD} = 0$) allows (47) to be expressed in the loop impedance plane as (48).

$$\begin{aligned} S'_{OP\_AG} &= r \bullet ZL1 - Z_{APP\_NLD} \\ S'_{POL\_AG} &= K_{SL0} \bullet ZS1 + Z_{APP\_NLD} \end{aligned} \tag{48}$$

In (48), K_{SL0} is equal to (49).

$$K_{SL0} = \frac{1 + K_{S0} \bullet K_C}{1 + K_0 \bullet K_C} \tag{49}$$

In (49), the zero-sequence compensation factor K_0 is provided by (13), and K_{S0} and K_C are as shown in (50) and (51).

$$K_{S0} = \frac{ZS0 - ZS1}{ZS1} \tag{50}$$

$$K_C = \frac{C0}{2 \bullet C1 + C0} \tag{51}$$

Keep in mind that the comparator in (48) for a single A-phase-to-ground fault is identical to the comparator for three-phase faults in (38), with the exception of the term K_{SL0} that multiplies ZS1.

Fig. 15 shows the variation of K_{SL0} when the fault is applied at a distance *d* varying from 0 to 1 pu and for a distance element installed at Bus L for the system in Fig. 6. Obviously, there is little variation in the magnitude and phase angle of K_{SL0}.

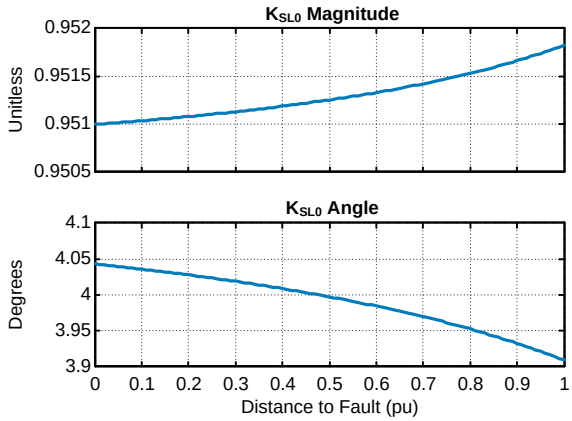

Fig. 15. Magnitude and phase angle of the coefficient K_{SL0} when the fault distance varies from 0 to 1 pu for the system in Fig. 6

2) Mho Element Characteristic for Single A-Phase-to-Ground Faults With PSV Polarization

When the polarizing voltage is equal to the PSV without any memory, the polarization becomes (52).

$$\begin{aligned} S_{OP\_AG} &= r \bullet ZL1 \bullet (IA + K_0 I0) - VA \\ S_{POL\_AG} &= VA1 \end{aligned} \tag{52}$$

The development for a single A-phase-to-ground fault is similar to that of a three-phase fault. The operating and polarizing quantities for the A-phase-to-ground fault loop in the impedance plane are shown in (53).

$$\begin{aligned} S'_{OP\_AG} &= r \bullet ZL1 - Z_{APP} \\ S'_{POL\_AG} &= ZS1 \bullet (K_{SL0} - K_{CC}) + Z_{APP} \end{aligned} \tag{53}$$

In (53), the variable K_{CC} is equal to (54).

$$K_{CC} = \frac{C1}{2C1 + C0(1 + K_0)} = \frac{C1 \bullet K_{RAG}}{3} \tag{54}$$

Fig. 16 shows the variation of ($K_{SL0} - K_{CC}$) for a distance element located at Bus L in Fig. 6 when a fault is applied a distance *d* varying from 0 to 1 pu. As expected, there is little variation in the magnitude and phase angle of the factor ($K_{SL0} - K_{CC}$).

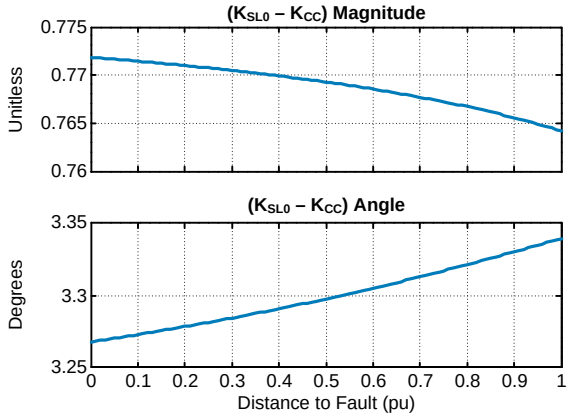

Fig. 16. Magnitude and phase angle of the coefficient ($K_{SL0} - K_{CC}$) when the fault distance varies from 0 to 1 pu for the system in Fig. 6

3) Incremental Distance Element Characteristic in the Impedance Plane for Single A-Phase-to-Ground Faults

Just as in the three-phase fault case, the prefault voltage at the fault location and the incremental voltage drop at the reach point for the single A-phase-to-ground loop are given by (55).

$$\begin{aligned} Ef_{AG} &= VA_{PF} - d \bullet ZL1 \bullet I_{LD} \\ Vd_{AG} &= -\Delta VA + r \bullet ZL1 \bullet \Delta IR_{AG} \end{aligned} \tag{55}$$

In (55), ΔIR_{AG} is equal to (56).

$$\Delta IR_{AG} = \Delta IA + K_0 \bullet I0 \tag{56}$$

Following the same procedure applied for the three-phase fault case provides (57) for an unloaded system.

$$\begin{aligned} Ef'_{AG} &= \frac{Ef_{AG}}{\Delta IR_{AG}} = K_{SL0} \bullet ZS1 + Z_{APP\_NLD} \\ Vd'_{AG} &= \frac{Vd_{AG}}{\Delta IR_{AG}} = K_{SL0} \bullet ZS1 + r \bullet ZL1 \end{aligned} \tag{57}$$

4) Comparison of Mho and Incremental Distance Element Characteristics for Single-Phase Faults

For distance elements installed at Bus L for the power system shown in Fig. 6, Fig. 17 plots the three distance element characteristics for faults in the middle of the line (d = 0.5 pu). Again, the incremental distance element is the one that exhibits the largest mho expansion.

Fig. 18 shows the resistance coverage of the mho element with PSV and PSVM polarizations and the incremental distance element. Again, the incremental distance element has the best coverage. Note that the conventional mho element with PSV polarization has a better resistance coverage than the same element applied to three-phase faults, as shown in Fig. 10. This is due to the fact that there is still PSV (provided by the two remaining healthy phases), even for a single A-phase-to-ground fault at the substation.

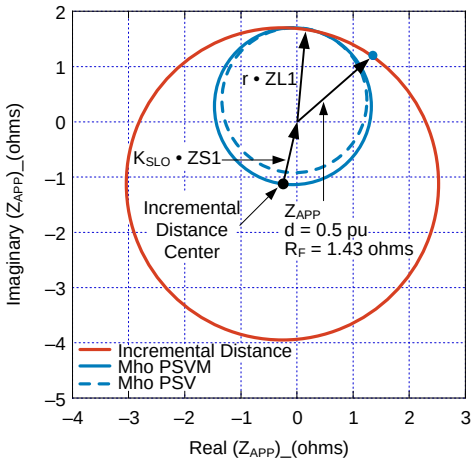

Fig. 17. Single-phase-to-ground fault mho and incremental distance element characteristics for a relay installed at Bus L of the network in Fig. 6 at d = 0.5 pu

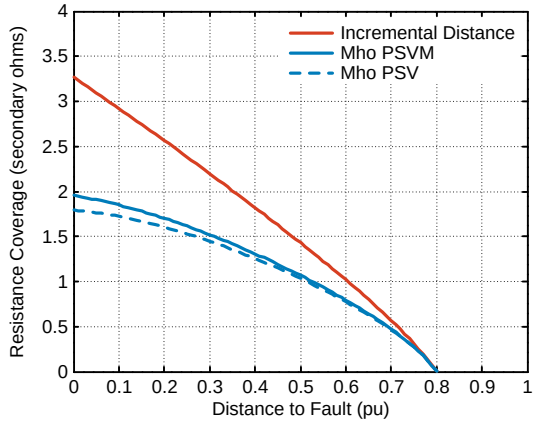

Fig. 18. Single A-phase-to-ground fault resistance coverage as a function of the distance to the fault

Fig. 18 shows that for the power system in Fig. 6, the maximum fault resistance for a fault 50 percent down the line from Bus L that the incremental distance element can detect is 1.43 ohms. The apparent impedance for the A-phase-to-ground fault is verified in (58).

$$\begin{aligned} &Z_{APP\_NLD}(d = 0.5,\ R_F = 1.43) = \\ &\frac{VA}{\Delta IA_{AG}} = d \bullet ZL1 + R_F \bullet K_{RAG} = (1.356 + j1.19)\ \Omega \end{aligned} \tag{58}$$

This apparent impedance is plotted in Fig. 17 and falls exactly on the incremental distance characteristic circle. Just as in the three-phase fault case, if the fault resistance is increased, the loop apparent impedance falls outside the characteristic circle.

C. Case of Phase-to-Phase Faults

1) Mho Element Characteristic for B-Phase-to-C-Phase and B-Phase-to-C-Phase-to-Ground Faults With PSVM Polarization

For a B-phase-to-C-phase fault, the operating and polarizing quantities with PSVM polarization for a conventional mho element can be expressed as (59).

$$\begin{aligned} S_{OP\_BC} &= r \bullet ZL1 \bullet (IB - IC) - (VB - VC) \\ S_{POL\_BC} &= VB1_{MEM} - VC1_{MEM} \end{aligned} \tag{59}$$

With an approach similar to the three-phase fault analysis and assuming a system with no load (I_{LD} = 0), (59) can be expressed in the loop impedance plane as (60).

$$\begin{aligned} S'_{OP\_BC} &= \frac{S_{OP}}{IBC} = r \bullet ZL1 - Z_{APP\_NLD} \\ S'_{POL\_BC} &= \frac{S_{POL}}{IBC} = ZS1 + Z_{APP\_NLD} \end{aligned} \tag{60}$$

This characteristic is the same as that of the three-phase faults in (38).

2) Mho Element Characteristic for B-Phase-to-C-Phase and B-Phase-to-C-Phase-to-Ground Faults With PSV Polarization

When the polarization voltage is equal to the PSV without any memory, (59) becomes (61).

$$\begin{aligned} S_{OP\_BC} &= r \bullet ZL1 \bullet (IB - IC) - (VB - VC) \\ S_{POL\_BC} &= VB1 - VC1 \end{aligned} \tag{61}$$

Just as in the previous three-phase fault case, the operating and polarizing quantities in the loop impedance plane are determined as shown in (62).

$$\begin{aligned} S'_{OP\_BC} &= r \bullet ZL1 - Z_{APP\_NLD} \\ S'_{POL\_BC} &= \frac{ZS1}{2} + Z_{APP\_NLD} \end{aligned} \tag{62}$$

The comparator in (62) for a phase-to-phase or phase-to-phase-to-ground fault is identical to the comparator for the three-phase fault in (38), with the exception of the divide by two term for ZS1.

3) Incremental Distance Element Characteristic in the Impedance Plane for B-Phase-to-C-Phase and B-Phase-to-C-Phase-to-Ground Faults

The prefault voltage and incremental voltage drop for the phase-to-phase B-phase-to-C-phase fault loop are provided by (63).

$$\begin{aligned} Ef_{BC} &= VA_{PF} \bullet (a^2 - a) - d \bullet I_{LD} \bullet (a^2 - a) \\ Vd_{BC} &= -(\Delta VB - \Delta VC) + r \bullet ZL1 \bullet (\Delta IB - \Delta IC) \end{aligned} \tag{63}$$

Finally, applying the same procedure as that for the three-phase fault case results in (64).

$$\begin{aligned} Ef'_{BC} &= \frac{Ef_{BC}}{\Delta IBC} = ZS1 + Z_{APP\_NLD} \\ Vd'_{BC} &= \frac{Vd_{BC}}{\Delta IBC} = ZS1 + r \bullet ZL1 \end{aligned} \tag{64}$$

Equation (64) is identical to the three-phase fault equation in (43).

4) Comparison of the Conventional Mho and Incremental Distance Element Characteristics for Phase-to-Phase Faults

The distance element characteristics in Fig. 19 for a relay installed at Bus L on the power system shown in Fig. 6 demonstrate that the incremental distance element once again provides the greatest expansion.

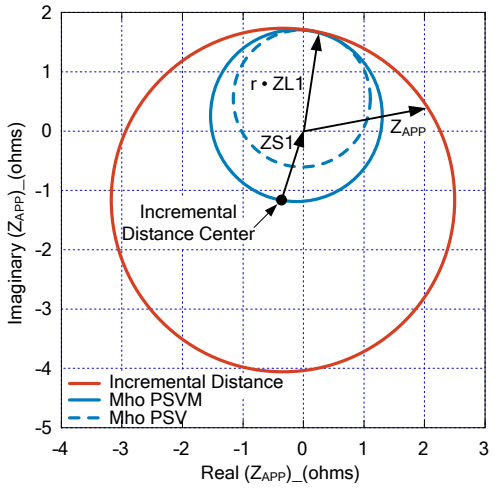

Fig. 19. Phase-to-phase fault mho and incremental distance element characteristics for a relay installed at Bus L of the network in Fig. 6

Fig. 20 shows the resistance coverage for all three elements; again, the incremental distance element provides the best resistance coverage.

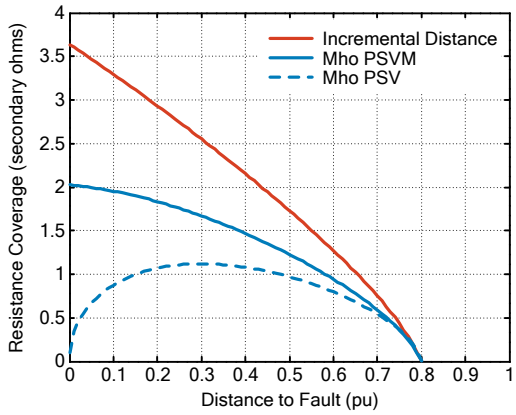

Fig. 20. B-phase-to-C-phase fault resistance coverage as a function of the distance to the fault

VI. Comparison Between Mho and Incremental Distance Element Characteristics

A. Characteristics comparison

When comparing Fig. 9, Fig. 17, and Fig. 19, it is clear that all three mho element characteristics with PSVM as the polarizing voltage for three-phase, single-phase, and double-phase faults are almost equal to one another. The same observation is true for the three corresponding characteristics of the incremental distance elements. The only characteristic that exhibits some significant change in its expansion is the conventional mho element with PSV polarization. In all cases, the conventional mho element with PSV always exhibits the smallest expansion of the mho element characteristic.

In all cases, the incremental distance element exhibits superior mho expansion when compared with the conventional mho element for all fault types, in the sense that they cover a larger area without overreaching in the loop impedance plane. This translates to better resistance coverage, and therefore increased sensitivity. Furthermore, the incremental distance element is immune to load. Section VIII explains that because the incremental distance element covers a larger portion of the impedance plane, which also includes the capacitive reactance, it allows this element to handle both voltage and current inversion when applied to series-compensated systems.

B. Limits of mho and incremental distance element modeling in this paper

The characteristics presented in this paper are derived from models that each include a single comparator. A single phase comparator is used to model the mho elements, and a single amplitude comparator is used to model the incremental distance elements. In reality, the single comparator for each element could be one among a few others in a practical implementation. Other potential conditions could include minimum signal levels for directional supervision or overcurrent supervision, and these conditions could affect the characteristics presented in this paper. This paper does not address the issue of the impact of these possible additional conditions.

VII. Implementation of Incremental Distance Element Using Delta Filters

A. The Base Delta Filter

In order to extract incremental voltage and current components, most applications have made use of so-called delta filters. The simplest form of a delta filter is represented in Fig. 21.

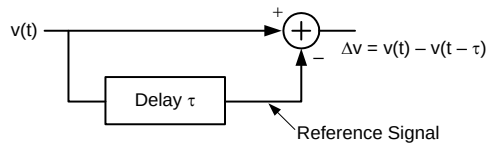

Fig. 21. Simple delta filter

Fig. 21 shows the original delta filter as applied to time varying signals (instantaneous quantities). The incremental quantity is obtained by subtracting the present instantaneous value (voltage or current) from the same quantity delayed by a time interval, typically equal to one power system cycle. The one-cycle-old signal (delayed signal) is the reference signal. The result of this calculation is the incremental change (Δ) as experienced by the input signal for a time interval equal to τ (τ determines the duration of the filter output for a disturbance to the input signal). During the steady-state condition defined by the constant magnitude and phase angle for voltages and currents, the output of the delta filter is zero. Typically, the delta filters are supervised by a disturbance detector that enables the delta filters should it detect a disturbance in the input signals. If the disturbance is due to a fault, the output of the delta filter corresponds to the change in voltage or current as a result of the fault for an interval of time equal to the delay τ. This change in voltage or current following a fault is commonly called the incremental voltage or current, or the superimposed component of voltage or current.

Fig. 21 represents an application where the incremental quantity calculation is performed in the time domain. Applications of delta filters in the time domain lead to elements typically operating at ultra-high speed [7]. The same delta filter could be applied in the frequency domain where the time signal v(t) is simply replaced by a phasor quantity that has been obtained from the output of a filter. Because of the filtering delay, operating times are slower than they would be if time-domain signals are used.

Conventional mho element implementation does not require the use of delta filters, and the element processing is continuous, so it does not require disturbance detectors.

B. Delta Filter Characteristics

1) Delta Filter Delay or Observation Window

Fig. 21 shows that the delay τ determines the output duration of the delta filter. The delay τ is therefore the time interval following the fault inception during which any element consuming incremental quantities is operational. This delay τ is typically between 1 to 2 power system cycles [1] [7] [8].

The operational availability of a conventional mho element is theoretically infinite. The only factor that could influence the operational availability of a conventional mho element is the availability of the PSVM polarization. For close-in three-phase faults, the requirement is that the PSVM must be available longer than the breaker failure time. In an application of series-compensated lines where voltage inversion is possible, the PSVM must be available longer than the operating time of the reverse-looking conventional mho distance element.

2) Delta Filter Reset Time

When applying the superposition principle as embodied in (3), it is necessary to define a new prefault voltage and current value every time a topological change has occurred on the power system. Practically, during a cascade of events that may occur over a short period of time, the nature of the delta filter is such that the succession of changes could become intractable. One solution to this issue is to block the delta filters for a brief interval of time, from a few cycles after a first event or fault has been detected to after the delay τ has expired. This interval of time corresponds to the delta filter reset time. Any function based on incremental quantities is not operational during the delta filter reset time.

Conventional mho elements do not have any reset time.

C. Limitations of Incremental Quantities

1) Lack of Signals During Switch on to Fault Situations

When a line is open and the line breaker is switched on an existing fault, measured prefault voltages and currents conditions are zero and do not correspond to the real prefault network values. During a switch on to fault situation, therefore, proper incremental quantities are not available.

The only limitation of the conventional mho element during switch on to fault situations is that only PSV is available, and PSVM polarization could be missing after the fault inception.

2) Incremental Quantities During Cascading Events

As explained previously, during a cascade of events, the delta filters could be in their reset time interval and the incremental quantities would not be available.

Conventional mho elements are normally not affected by cascading events.

3) Evolving Faults

An evolving fault is a fault for which the fault type changes with time. For example, a fault could evolve from A-phase-to-ground to A-phase-to-B-phase-to-ground. Evolving faults that evolve with a time span greater than the delay τ are not detected by elements that consume incremental quantities.

Conventional mho elements are not affected by evolving faults and should be able to track them.

D. Interpretation of the Distance Element Characteristic in the Loop Impedance Plane

In order for any incremental distance element characteristic in the loop impedance plane to exist, it is necessary that the corresponding voltage and current incremental quantities be

different from zero. Whether the network is heathy or faulted, the output of a delta filter is zero in steady state. Following a fault, incremental quantities are non-zero only during an interval of time equal to the filter delay τ. It is only during this interval of time that the element characteristic in the impedance plane exists and that the location check of the apparent impedance can be performed. As explained previously, the conventional mho element characteristics in the impedance plane always exist.

In steady state, when the incremental quantities are zero by definition, situations can develop where the apparent impedance of a particular impedance loop is inside a mho element characteristic and the mho element asserts. Because an incremental distance element characteristic is not defined in steady state, this element does not assert in the same situation.

A good example of the proposition in the previous paragraph is an apparent impedance that is sitting still inside a phase mho element characteristic because of an overload condition. The mho element asserts, but the phase incremental distance elements do not pick up because the system is in steady state.

E. Speed of Functions Based on Incremental Quantities

The technological trend has been to design incremental quantities-based functions and, particularly, incremental distance elements with operation time of a few milliseconds to less than one cycle [1] [7] [8]. Under these conditions, incremental distance elements are typically supplemented by slower, more dependable conventional mho elements. The combination of the two is arguably optimal in terms of speed and dependability.

VIII. Mho and Incremental Distance Elements With Series-Compensated Lines

Three well-known difficulties are associated with the application of distance elements to the protection of series-compensated lines: Zone 1 overreaching, voltage inversion, or current inversion [9] [10]. Consider the system shown in Fig. 22 as an example. Note that the relay voltages are measured at Bus L behind the capacitor and that the fault distance is taken from the capacitor outer extremity to the fault point on the line.

In Fig. 22, impedances are shown in primary values, but secondary values are used throughout the text and for all other figures.

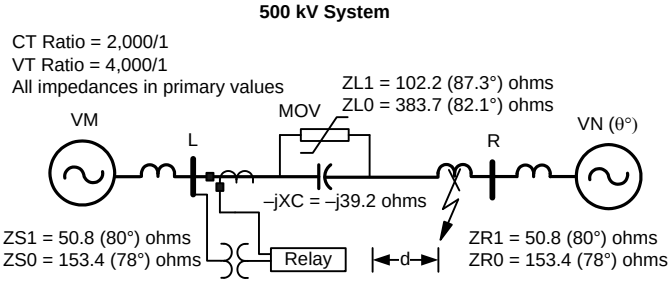

Fig. 22. Series-compensated, 500 kV network

A. Capacitor-MOV Equivalent Circuit

It has been demonstrated in [11] that the combination of a series capacitor with a metal-oxide varistor (MOV) in parallel can be represented by the linearized equivalent impedance of a resistance in series with a capacitance, as shown in Fig. 23. The values of the equivalent resistance and capacitor depend on the current IC flowing in the equivalent impedance. For the system shown in Fig. 22, Fig. 24 and Fig. 25 show the measured equivalent capacitance and resistance as a function of the fault secondary current. These plots have been obtained by calculating the ratio of the fundamental voltage phasor across the capacitor over the fundamental current phasor for different current fault levels.

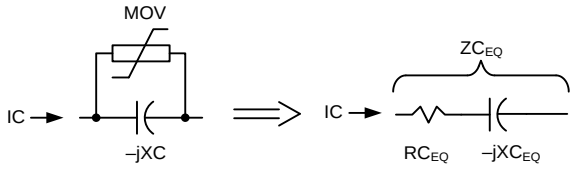

Fig. 23. Series capacitor equivalent circuit

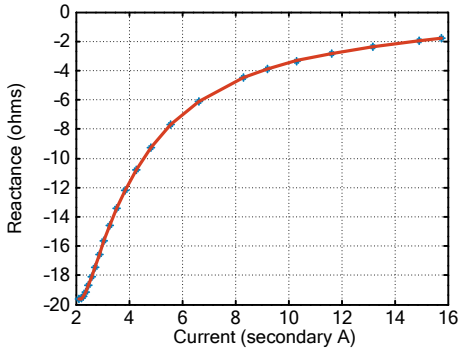

Fig. 24. Equivalent capacitance XC_{EQ} as a function of secondary current

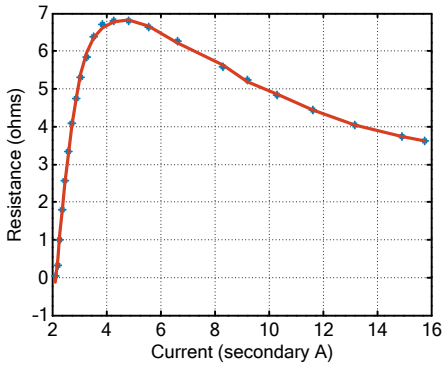

Fig. 25. Equivalent resistance RC_{EQ} as a function of secondary current

B. Sequence Network of Series-Compensated Circuit

In order to derive the characteristic of either a conventional mho or incremental distance element in the loop impedance plane, it is necessary to build the fault sequence network. When it comes to a network similar to Fig. 22 with series compensation, [9] has demonstrated that this can be done only if the capacitor value is the same for all three phases. Otherwise, coupling develops between the positive-sequence, negative-sequence, and zero-sequence networks. The

following two conditions exist for which all three phases see the same capacitor value:

- The MOV is removed. Therefore, the capacitor in each sequence network is equal to the original capacitor value.
- The MOV is operating and a three-phase fault is applied. The capacitor in the positive-sequence network is equal to the equivalent impedance ZC_{EQ}, which varies with the fault current.

Fig. 26 shows the pure-fault sequence network for a three-phase fault on the network shown in Fig. 22. The voltages and currents of this circuit can be resolved using an iterative technique in order to take into account the nonlinearity of the equivalent resistance and capacitance as provided by the plots shown in Fig. 24 and Fig. 25. RC_{EQ} and XC_{EQ} are changed iteratively until their calculated values correspond to the computed fault current.

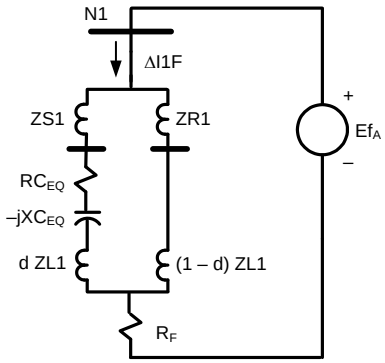

Fig. 26. Pure-fault sequence network for three-phase fault on network in Fig. 22

C. Zone 1 Overreaching

The overreaching issue associated with Zone 1 of a conventional mho element is also present in incremental distance elements. The same Zone 1 pull-back solution applied to conventional mho elements has to be applied to incremental distance elements. This is demonstrated by resolving the sequence network of Fig. 26 for a three-phase fault located at distance *d*, which varies from 0 to 1 pu. Two Zone 1 reach settings are tested at 40 and 80 percent of the line length. Fig. 27 shows the secondary fault current as the fault distance moves from 0 to 100 percent of the line length. The fault current determines XC_{EQ} and RC_{EQ} for the capacitor-MOV combination, as provided by Fig. 24 and Fig. 25.

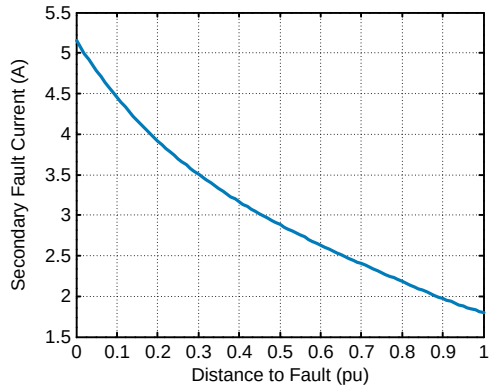

Fig. 27. Three-phase fault current as a function of the distance to the fault

Fig. 28 shows the scalar product relative to the mho AB impedance loop. Obviously, with a reach of 80 percent, the mho element overreaches for a fault at 100 percent because the scalar product is positive. With the Zone 1 reach set at 40 percent, the mho element covers a little less than 80 percent of the line.

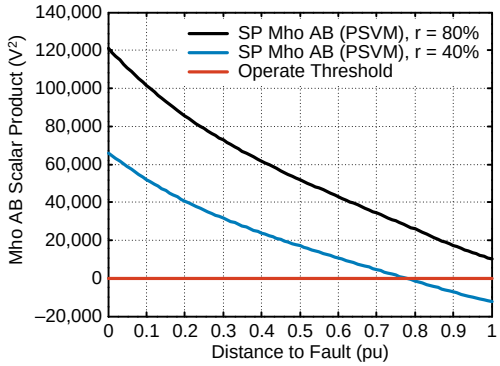

Fig. 28. AB loop mho element scalar product with reach equal to 40 and 80 percent of ZL1 as a function of the distance to the fault

Fig. 29 shows the performance of the AB incremental distance element. For a fault at 100 percent and a Zone 1 reach of 80 percent, the incremental element is overreaching because Vd_{AB} is greater than Vf_{AB}. With a Zone 1 reach set at 40 percent, the element covers a little less than 80 percent of the line. This example illustrates that the incremental distance element Zone 1 reach has to be reduced in the same proportion as the conventional mho elements.

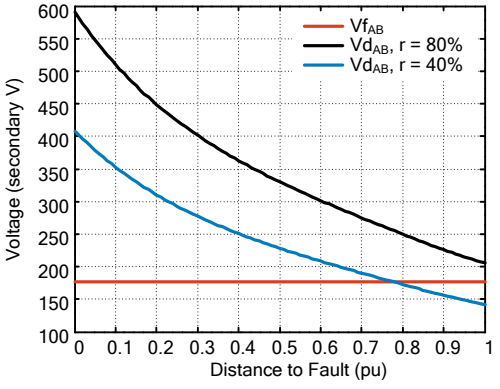

Fig. 29. AB loop incremental distance Vf_{AB} and Vd_{AB} with reach equal to 40 and 80 percent of ZL1

D. Voltage Inversion

For a system similar to that of Fig. 22, voltage inversion is traditionally defined as the condition that takes place when the inequalities in (65) are true [10].

$$\begin{aligned} \left|ZC_{EQ}\right| &> \left|d \bullet ZL1\right| \\ \left|ZS1 + d \bullet ZL1\right| &> \left|ZC_{EQ}\right| \end{aligned} \tag{65}$$

Equation (65) embodies the principle that the impedance between the relaying point and the fault point is capacitive, but the overall impedance between the source behind the relay and the fault point is still inductive.

The most onerous condition develops if a three-phase fault is applied at distance d = 0 with the MOV removed. The loop apparent impedance is simply equal to the capacitive reactance, as shown in (66).

$$Z_{APP} = -jXC \tag{66}$$

Fig. 30 shows the location of the loop apparent impedance relative to the three-phase mho and incremental distance element characteristics when a three-phase fault is applied at distance d = 0 for the system in Fig. 22 and where the Zone 1 reach is set to 50 percent of the line length.

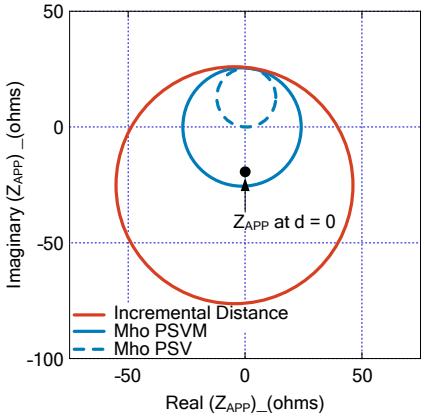

Fig. 30. Three-phase fault loop apparent impedance with voltage inversion for fault applied at d = 0 with original source impedance ZS1, MOV removed, and a reach of 50 percent

Both the conventional mho distance element with PSVM polarization and the incremental distance element detect this fault (due to mho expansion). Only the conventional mho element with PSV polarization fails to detect the fault because its characteristic does not expand sufficiently enough to detect this type of fault.

E. Current Inversion

For the system shown in Fig. 22, current inversion occurs when the condition in (67) is met [10].

$$\left|ZC_{EQ}\right| > \left|ZS1 + d \bullet ZL1\right| \tag{67}$$

Equation (67) embodies the principle that the overall impedance between the source behind the relay and the fault point is capacitive.

For the system in Fig. 22, the source impedance ZS1 is divided by two in order to create a condition for current inversion. As for the voltage inversion case, the most onerous condition develops with a three-phase fault at distance d = 0 with the MOV removed. The loop apparent impedance then corresponds again to (66). Fig. 31 shows the location of the loop apparent impedance relative to the three distance elements, conventional mho elements, and incremental distance element characteristics. The incremental distance element is the only one that detects the fault. This confirms the well-established fact that the mho element with PSVM polarization cannot normally handle current inversion. Note that the incremental distance element has no problem with current inversion.

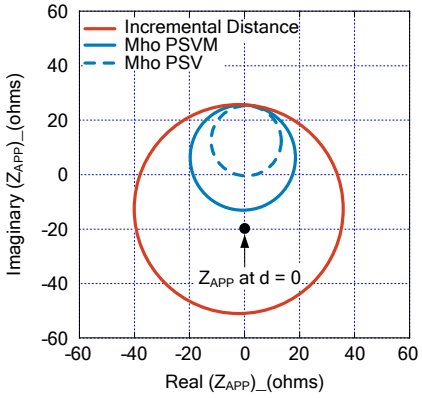

Fig. 31. Three-phase fault loop apparent impedance with current inversion for a fault applied at d = 0 with source impedance divided by 2, MOV removed, and a reach of 50 percent

F. Example of Three-Phase Faults

The sequence network shown in Fig. 26 is used to resolve cases of three-phase faults. The source impedance behind the relay (ZS1) is again divided by two so as to have a system that is more prone to current inversion. The three-phase faults are applied in front of the relay terminal (d = 0) with increasing values for R_F. All of the distance element reaches *r* are set to 50 percent of the line length.

For a no-load condition, the apparent impedance (Z_{APP_NLD}) as seen by a phase impedance loop is demonstrated in (68).

$$Z_{APP\_NLD} = d \bullet ZL1 + ZC_{EQ} + \frac{R_F}{C1} \tag{68}$$

The current distribution factor of (5) now becomes (69).

$$C1_{SER} = \frac{(1-d) \bullet ZL1 + ZR1}{ZS1 + ZR1 + ZL1 + ZC_{EQ}} \tag{69}$$

Fig. 32 shows the locations of the apparent impedances for increasing R_F together with the characteristics of the three distance elements if the relay were located at Bus L in Fig. 22. The conventional mho element with PSV polarization does not detect any of the faults. The conventional mho elements with PSVM polarization detect the faults up to a fault resistance R_F of 6 ohms. The phase incremental distance elements detect faults with R_F up to 34 ohms. Contrary to the case shown in Fig. 31, where the MOV was removed and the fault with current inversion was not detected by the mho element with PSVM polarization, the same element now detects the fault with zero resistance because the equivalent capacitor XC_{EQ} is substantially reduced compared with XC due to the presence of the MOV and the high fault current (see Fig. 24).

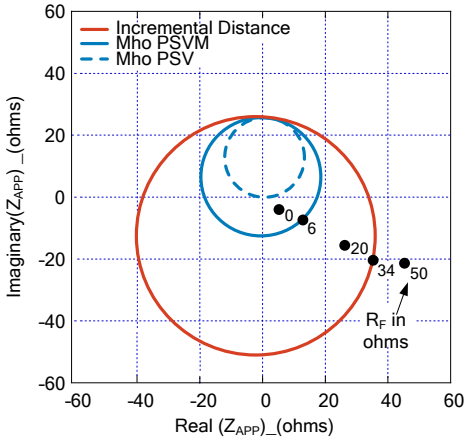

Fig. 32. Location of apparent impedances as a function of the fault resistance for three-phase faults applied at d = 0

Fig. 33 shows variations of the AB loop incremental quantities Vf_{AB} and Vd_{AB} as a function of the fault resistance R_F. Vd_{AB} is greater than Vf_{AB} up to a resistance of 34 ohms. This is consistent with the Fig. 32 plot, which shows the apparent impedance with a resistance of 34 ohms right on the incremental distance three-phase fault characteristic.

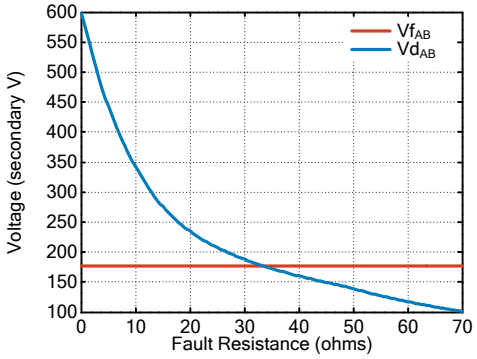

Fig. 33. AB loop incremental quantities Vf_{AB} and Vd_{AB} for a three-phase fault at d = 0 as a function of fault resistance

Fig. 34 shows the variation of the mho AB scalar products with PSVM and PSV polarizations. Obviously, the scalar product relative to the mho AB loop with PSV polarization never becomes positive. That corresponds in Fig. 32 to the apparent impedances that are never inside the blue dashed line characteristic. The mho AB scalar product with PSVM polarization is positive up to a fault resistance of about 6 ohms. This is consistent with Fig. 32, which shows the apparent impedance with a 6-ohm resistance right above the blue line characteristic.

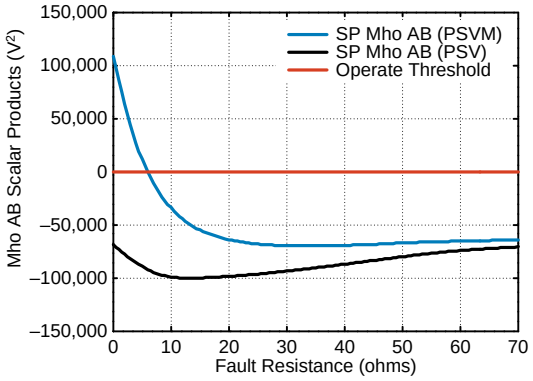

Fig. 34. Mho AB scalar products with PSVM and PSV polarizations for a three-phase fault at d = 0 as a function of fault resistance

Fig. 35 shows the variation of the resistance coverage for all three distance elements as the distance to the fault varies from 0 to 1 pu. The superiority of the incremental distance elements in terms of sensitivity and resistance coverage is again demonstrated.

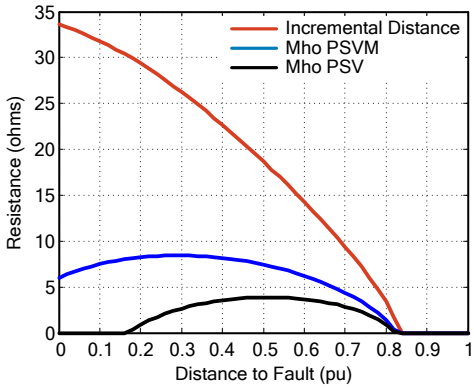

Fig. 35. Resistance coverage for three-phase faults as a function of the distance to the fault for the network in Fig. 22 with ZS1 divided by 2

IX. Case of Reverse and Resistive Three-Phase Faults

Three cases exist where the reliability of mho elements with PSV polarization is particularly challenged and the risk of a misoperation is high. They are as follows:

- Series-compensated lines with voltage inversion.
- Three-phase bolted faults.
- Resistive and reverse three-phase faults.

In order to illustrate the third case, Fig. 36 shows the maximum fault resistance R_F that can be covered by conventional mho and incremental distance elements as a function of the reverse reach (in pu of the line length). The plots were obtained for the network in Fig. 6, where reverse three-phase faults are applied behind Bus L and the terminal imports power in steady state (VM has a phase angle lag of 15 degrees with respect to VN). Obviously, the conventional mho element with PSV polarization does not perform well with an R_F coverage close to zero [5]. The mho element with PSVM polarization does much better, and finally, the incremental distance exhibits superior performance. The plots indicate that the higher the reach, the higher the R_F coverage for both the conventional mho element with PSVM polarization and the incremental distance element.

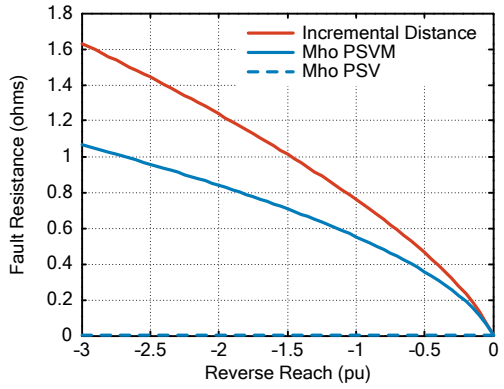

Fig. 36. Resistance coverage as a function of reverse reach for three-phase faults applied behind Bus L of the network in Fig. 6

X. Impact of Remote Infeed (or Outfeed) on the Distance Element Reach

This section demonstrates that the underreaching effect due to remote infeed equally affects both the conventional mho element and the incremental distance element. In order to illustrate this, the three-terminal system shown in Fig. 37 has been created. The circuit in Fig. 37 is identical to the circuit in Fig. 6, with the exception of the added feeder and source. The T-point is exactly at 50 percent of the original line length. A three-phase fault is applied on the line, with the fault distance varying from 0 to 1 pu and the distance element reach set at 80 percent.

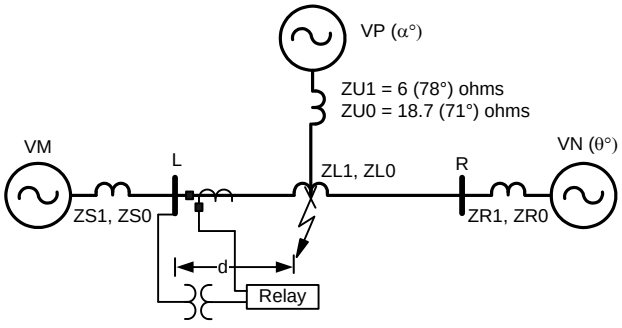

Fig. 37. Addition of a feeder to the system in Fig. 6

Fig. 38 shows the AB loop mho scalar product, which exhibits a discontinuity point at distance d = 50 percent, as expected. Past this distance, the element starts to underreach because of the infeed. The element detects the fault up to 57 percent of the line length. Fig. 39 shows the plot of Vf_{AB} and Vd_{AB} and shows that the incremental distance behaves exactly as the conventional mho element. The amount of underreach is identical.

In Fig. 38 and Fig. 39, the plots of the mho AB scalar product and Vd_{AB}, respectively, could be exactly superposed if the scaling were adjusted. This result should not be surprising, because for both elements, mho and incremental distance, the detection principles are based on the same equation, which is (8) in this paper. Similar conclusions can be reached with a remote outfeed.

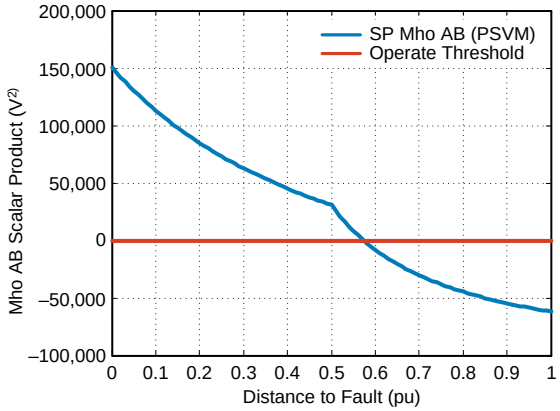

Fig. 38. AB loop mho element scalar product with reach of 80 percent for a three-phase fault applied from distance 0 to 1 pu

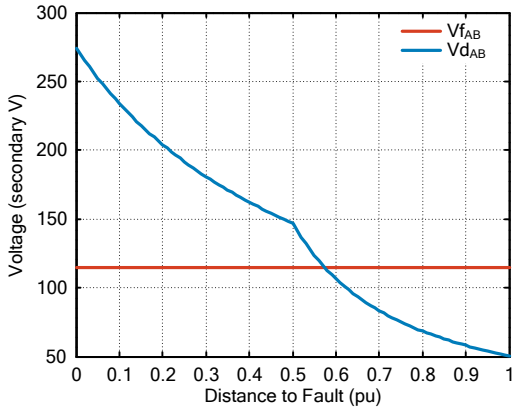

Fig. 39. AB loop incremental distance Vf_{AB} and Vd_{AB} with a reach of 80 percent for a three-phase fault applied from distance 0 to 1 pu

XI. Impact of Parallel Line With Mutual Coupling on Distance Element Reach

The principle described in the previous section can be applied in the case of parallel lines with mutual coupling: mho and incremental distance elements are affected in their underreaching or overreaching conditions in the same proportion, and the compensating principles to remove these problems are exactly the same for both distance elements.

In order to illustrate this, a double circuit line has been created using the same network as in Fig. 6 and is shown in Fig. 40. An identical line has been added in parallel, and the mutual impedance ZM0 has been set to 0.9 times the original ZL0. A single A-phase-to-ground fault is applied from distance 0 to 1 pu. The distance element reach is set at 80 percent.

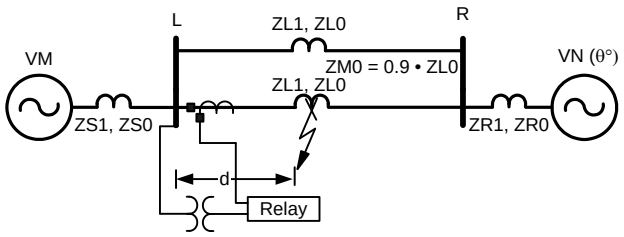

Fig. 40. Parallel lines circuit based on network in Fig. 6

Fig. 41 shows the variation of the AG loop incremental distance quantities Vf_{AG} and Vd_{AG} as a function of the distance to the fault. When no compensation is applied (Vd_{AG} in black trace), the element underreaches and covers up to 70 percent of the line length. When compensation is applied (Vd_{AG} in blue trace), the element covers 80 percent of the line as expected. The compensation consists of adding the adjacent line zero-sequence current correction to the quantity Vd_{AG}, as would be done with a mho element, as shown in (70) [12].

$$Vd_{AG} = -\Delta VA + r \bullet ZlL \bullet (\Delta IA + K_0 \bullet I0 + I0_{adj} \bullet \frac{ZM0}{ZL1}) \quad (70)$$

This compensation type is normally not recommended because of its lack of practicality. It is used here only as an illustration because it provides a perfect mathematical compensation with zero error. As indicated in [12], a better compensation is the correction of the zero-sequence compensating factor K_0.

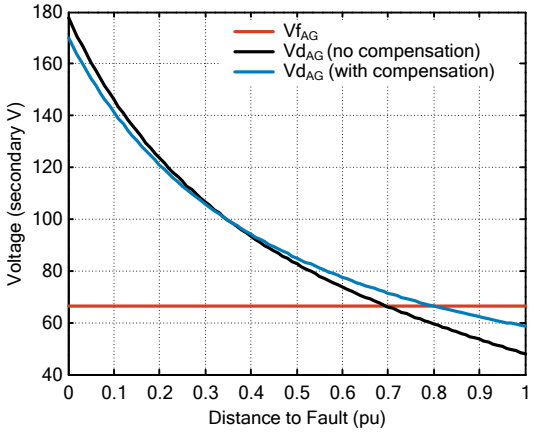

Fig. 41. AG loop incremental distance Vf_{AG} and Vd_{AG} with a reach of 80 percent for a single-phase fault applied from distance 0 to 1 pu

Fig. 42 shows the scalar products of the AG loop mho element with and without compensation. Without compensation, the mho element underreaches in the same proportion as the incremental distance. The same compensation has been applied to the operating quantity of the mho element in (71).

$$S_{opAG} = r \bullet ZL1 \bullet (IA + K_0 \bullet I0 + I0_{adj} \frac{ZM0}{ZL1}) - VA \quad (71)$$

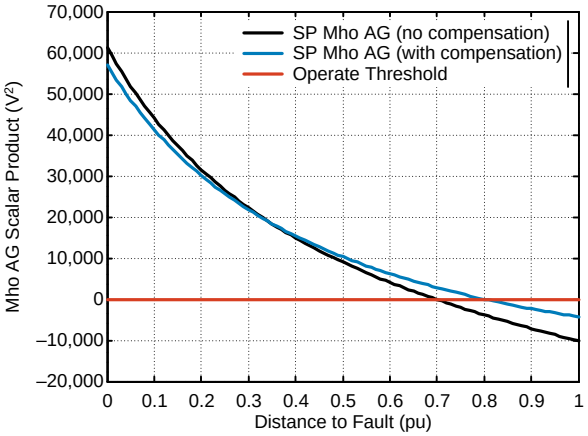

Fig. 42. AG loop mho scalar products with a reach of 80 percent for a single-phase fault applied from distance 0 to 1 pu

The same comment can be made for this case as was made for the remote infeed case: the plots in Fig. 41 and Fig. 42 could be exactly superposed if the scaling was adjusted. Again, this is proof that both distance elements, mho and incremental distance, use the same base equation in reality. This is (12) for single-phase-to-ground faults.

XII. Conclusion

A fundamental difference between the characteristics in the impedance plane of the mho and incremental distance elements is that characteristics of incremental distance elements exist only if the corresponding incremental voltages and currents are non-zero. They are not defined in steady state.

This paper shows that incremental distance elements exhibit characteristics in the loop impedance planes that have a larger intrinsic expansion than the ones shown with the maximum expansion of corresponding mho elements. As a consequence, incremental distance elements have better sensitivity and resistance coverage superior to corresponding mho elements.

Because their characteristics cover a larger area in the capacitive reactance zone of the loop impedance plane and because of the inherent memory present with incremental distance elements, they also have a better and intrinsic capability to cope with voltage or current inversion when applied to series-compensated line protection.

This paper demonstrates that the element reach for both mho and incremental distance elements is affected in the same proportions when it comes to Zone 1 with series compensation, remote infeed or outfeed, and, finally, parallel lines with mutual coupling. The same techniques to cope with conventional mho element issues can be applied to incremental distance elements.

If it were not for the limitations imposed by the delta filters in terms of an essentially reduced observation window, incremental distance elements would constitute a better choice as distance elements compared with mho elements. Because of these limitations, the technological trend has been to use them for the implementation of high or ultra-high speed distance elements where they are supplemented in parallel by slower conventional mho elements.

XIII. References

[1] G. Benmouyal and J. Roberts, "Superimposed Quantities: Their True Nature and Their Application in Relays," proceedings of the 26th Annual Western Protective Relay Conference, Spokane, WA, October 1999.

[2] G. Benmouyal, A. Guzmán, and R. Jain, "Tutorial on the Impact of Network Parameters on Distance Element Resistance Coverage," proceedings of the 40th Annual Western Protective Relay Conference, Spokane, WA, October 2013.

[3] R. J. Marttila, "Directional Characteristics of Distance Relay Mho Elements: Part I – A New Method of Analysis," *IEEE Transactions on Power Apparatus and Systems*, Vol. PAS-100, No. 1, February 1981, pp. 96–102.

[4] R. J. Marttila, "Directional Characteristics of Distance Relay Mho Elements: Part II – Results," *IEEE Transactions on Power Apparatus and Systems*, Vol. PAS-100, No. 1, February 1981, pp. 103–113.

[5] E. O. Schweitzer, III and J. Roberts, "Distance Relay Element Design," proceedings of the 46th Annual Conference for Protective Relay Engineers, College Station, TX, April 1993.

[6] D. D. Fentie, "Understanding the Dynamic Mho Distance Characteristic," proceedings of the 69th Annual Conference for Protective Relay Engineers, College Station, TX, April 2016.

[7] E. O. Schweitzer, III, B. Kasztenny, A. Guzmán, V. Skendzic, and M. V. Mynam, "Speed Of Line Protection – Can We Break Free of Phasor Limitations?" proceedings of the 68th Annual Conference for Protective Relay Engineers, College Station, TX, March 2015.

[8] E. O. Schweitzer, III, B. Kasztenny, and M. V. Mynam, "Performance of Time-Domain Line Protection Elements on Real-World Faults," proceedings of the 69th Annual Conference for Protective Relay Engineers, College Station, TX, April 2016.

[9] B. Kasztenny, "Distance Protection of Series Compensated Lines – Problems and Solutions," proceedings of the 28th Annual Western Protective Relay Conference, Spokane, WA, October 2001.

[10] E. Bakie, C. Westhoff, N. Fischer, and J. Bell, "Voltage and Current Inversion Challenges When Protecting Series-Compensated Lines – A Case Study," proceedings of the 69th Annual Conference for Protective Relay Engineers, College Station, TX, April 2016.

[11] D. L. Goldsworthy, "A Linearized Model for MOV-Protected Series Capacitors," *IEEE Transactions on Power Systems*, Vol. 2, No. 4, December 1987, pp. 953–957.

[12] D. A. Tziouvaras, H. J. Altuve, and F. Calero, "Protecting Mutually Coupled Transmission Lines: Challenges and Solutions," proceedings of the 67th Annual Conference for Protective Relay Engineers, College Station, TX, March 2014.

XIV. Biographies

Gabriel Benmouyal, P.E., received his BASc in electrical engineering and his MASc in control engineering from Ecole Polytechnique, Université de Montréal, Canada. In 1978, he joined IREQ, where his main fields of activity were the application of microprocessors and digital techniques for substations and generating station control and protection systems. In 1997, he joined Schweitzer Engineering Laboratories, Inc. as a principal research engineer. Gabriel is a registered professional engineer in the Province of Québec and an IEEE senior member and has served on the Power System Relaying Committee since May 1989. He holds more than six patents and is the author or coauthor of several papers in the fields of signal processing and power network protection and control.

Normann Fischer received a Higher Diploma in Technology, with honors from Technikon Witwatersrand, Johannesburg, South Africa, in 1988; a BSEE, with honors, from the University of Cape Town in 1993; a MSEE from the University of Idaho in 2005; and a PhD from the University of Idaho in 2014. He joined Eskom as a protection technician in 1984 and was a senior design engineer in the Eskom protection design department for three years. He then joined IST Energy as a senior design engineer in 1996. In 1999, Normann joined Schweitzer Engineering Laboratories, Inc., where he is currently a fellow engineer in the research and development division. He was a registered professional engineer in South Africa and a member of the South African Institute of Electrical Engineers. He is currently a senior member of IEEE and a member of the American Society for Engineering Education (ASEE).

Brian Smyth received a BSEE and MSEE from Montana Tech at the University of Montana in 2006 and 2008, respectively. He joined Montana Tech as a visiting professor in 2008 and taught classes in electrical circuits, electric machinery, instrumentation and controls, and power system analysis. He joined Schweitzer Engineering Laboratories, Inc. in 2009 as an associate power engineer in the research and development division. Brian is a lead product engineer in the transmission and substation group. He is a coauthor of several papers on battery impedance measurement and power system out-of-step conditions. He is also an active IEEE member and a registered professional engineer in the state of Washington.

Previously presented at the 2017 Texas A&M Conference for Protective Relay Engineers.

20170130 • TP6769-01